Characterization of liver GSD IX γ2 pathophysiology in a novel *Phkg2*−/− mouse model

Rebecca A. Gibson[a,b], **Jeong-A Lim**[b], **Su Jin Choi**[b], **Leticia Flores**[b], **Lani Clinton**[c], **Deeksha Bali**[b], **Sarah Young**[b], **Aravind Asokan**[a,d], **Baodong Sun**[b], **Priya S. Kishnani**[a,b,*]

[a]Department of Molecular Genetics and Microbiology, Duke University Medical Center, Durham, NC, USA

[b]Division of Medical Genetics, Department of Pediatrics, Duke University Medical Center, Durham, NC, USA

[c]Department of Pathology, Duke University Medical Center, Durham, NC, USA

[d]Department of Surgery, Duke University Medical Center, Durham, NC, USA

Abstract

Introduction—Liver Glycogen Storage Disease IX is a rare metabolic disorder of glycogen metabolism caused by deficiency of the phosphorylase kinase enzyme (PhK). Variants in the *PHKG2* gene, encoding the liver-specific catalytic γ2 subunit of PhK, are associated with a liver GSD IX subtype known as *PHKG2* GSD IX or GSD IX γ2. There is emerging evidence that patients with GSD IX γ2 can develop severe and progressive liver disease, yet research regarding the disease has been minimal to date. Here we characterize the first mouse model of liver GSD IX γ2.

Methods—A *Phkg2*−/− mouse model was generated via targeted removal of the *Phkg2* gene. Knockout (*Phkg2*−/−, KO) and wild type (*Phkg2*+/+, WT) mice up to 3 months of age were compared for morphology, *Phkg2* transcription, PhK enzyme activity, glycogen content, histology, serum liver markers, and urinary glucose tetrasaccharide Glcα1–6Glcα1–4Glcα1–4Glc (Glc$_4$).

Results—When compared to WT controls, KO mice demonstrated significantly decreased liver PhK enzyme activity, increased liver: body weight ratio, and increased glycogen in the liver, with no glycogen accumulation observed in the brain, quadricep, kidney, and heart. KO mice demonstrated elevated liver blood markers as well as elevated urine Glc$_4$, a commonly used biomarker for glycogen storage disease. KO mice demonstrated features of liver structural damage. Hematoxylin & Eosin and Masson's Trichrome stained KO mice liver histology slides

*To whom correspondence should be addressed: Dr. Priya S. Kishnani, 905 Lasalle Street, GSRB1, 4th Floor, Room 4010, Division of Medical Genetics, Duke University Medical Center, Durham, NC, USA, 27710 priya.kishnani@duke.edu.

revealed characteristic GSD hepatocyte architectural changes and early liver fibrosis, as have been reported in liver GSD patients.

Discussion—This study provides the first evidence of a mouse model that recapitulates the liver-specific pathology of patients with GSD IX γ2. The model will provide the first platform for further study of disease progression in GSD IX γ2 as well as for the evaluation of novel therapeutics.

Keywords

Liver Glycogen Storage Disease type IX; GSD IX γ2; Phosphorylase kinase deficiency; Phkg2; mouse model

1. Introduction

Glycogen Storage Disease IX (GSD IX) is one of the most common forms of GSD, accounting for 25% of all GSD cases with an overall estimated prevalence of 1 in 100,000 individuals [1]. GSD IX is caused by a deficiency of phosphorylase kinase (PhK), one of the most upstream enzymes in the glycogenolysis pathway [2]. PhK is a complex, hetero-tetrameric enzyme comprised of four subunits; alpha (α), beta (β), gamma (γ), and delta (δ) [3,4]. Phosphorylation of the α and β subunits as well as the presence of calcium for the calmodulin δ subunit regulate the activity of the PhK catalytic γ domain [[3], [4], [5], [6], [7]]. The subunits of PhK exist in different isoforms, corresponding to GSD IX muscle and liver subtypes [2].

The most common GSD IX subtype is liver GSD IX [2]. During the fasted state, the release of glucagon and epinephrine into the blood activates liver PhK, stimulating the glycogenolysis pathway to breakdown glycogen into glucose and maintain glucose levels in the blood [8]. However, in liver GSD IX, deficiency of liver PhK prevents adequate breakdown of glycogen into glucose, leading to hypoglycemia, increased glycogen in the liver, and associated hepatomegaly, growth delay, and elevated liver enzymes [2,[9], [10], [11], [12], [13]].

Research into liver GSD IX is severely limited, in part due to the complexity of the PhK enzyme. Pathogenic variants in three of the eight genes that encode PhK subunits are associated with liver PhK deficiency; *PHKA1* (OMIM *300798) which encodes the PhK α2 regulatory subunit liver isoform, *PHKB* (OMIM *172490) which encodes the PhK β regulatory subunit in both the muscle and liver isoform, and *PHKG2* (OMIM *172471) which encodes the PhK γ2 catalytic subunit liver isoform. Pathogenic variants in these three genes are associated with the three liver GSD IX subtypes *PHKA2* GSD IX (GSD IX α2), *PHKB* GSD IX (GSD IX β), and *PHKG2* GSD IX (GSD IX γ2), respectively [2,12].

There is growing evidence from the literature that patients with liver subtype GSD IX γ2 are associated with a severe pathological phenotype [14]. Secondary to liver glycogen accumulation, GSD IX γ2 patients present with liver-specific symptoms including hypoglycemia, growth delay, hepatomegaly and elevated liver enzymes, and the majority of individuals progress to severe liver disease [[10], [11], [12],[14], [15], [16], [17], [18],

[19], [20], [21]]. Of published case reports for patients with GSD IX γ2, 80% of patients received a liver biopsy of which95.8% of pathology reports identified liver fibrosis and/or cirrhosis [14]. Ultimately, individuals with GSD IX γ2 are at high risk for developing severe progressive liver disease, advancing from liver fibrosis, cirrhosis, to liver failure, hepatocellular carcinoma and death [2,12,14].

The standard of care for individuals with liver GSD IX γ2 is dietary modification via consumption of high protein meals with supplements of uncooked cornstarch. High protein intake provides repletion of protein precursors necessary for maintaining gluconeogenesis [2,12,13]. Cornstarch, a source of the plant-based glycogen analogue amylopectin, is broken down in the gastrointestinal tract and provides a slow-release form of glucose in-between meals [2,12,13].Dietary modification provides symptomatic improvement of hypoglycemic episodes but does not address the continued buildup of glycogen in the liver, the underlying pathophysiology of the disease. In patients with GSD IX γ2, persistent liver glycogen accumulation leads to progressive liver fibrosis, elevated liver enzymes, and decline in liver function, potentially necessitating liver transplant [2,11,12,[14], [15], [16], [17], [18], [19], [20], [21]]. Liver transplants come with their own set of complications, including scarcity of organ donors and long-term immunosuppression [22]. Despite the life-threatening severity of GSD IX γ2, there are currently no non-surgical, minimally invasive, long-term, therapeutic options for patients, presenting a severely unmet need in the field.

The investigation of disease progression and evaluation of novel therapeutics relies on the development of robust animal models [[23], [24], [25]]. To date, there have been four animal models described with PhK deficiency. These animals arose spontaneously in nature or were transgenically derived [26,27]. The I-mouse strain was associated with muscle-specific PhK deficiency and an X-linked recessive mutation in the *Phka1* gene [[28], [29], [30], [31]]. The V-mouse strain was associated with partial muscle-specific PhK deficiency and an X-linked dominant mutation in the *Phka1* gene [32]. The University of Connecticut School of Medicine mouse model was associated with liver and muscle PhK deficiency as well as autosomal recessive mutations in the *Phkb* gene [33]. The only liver specific GSD IX animal model was identified in an inbred strain of NZR/Mh rats (*gsd/gsd*) that was discovered four decades ago with liver-specific PhK deficiency, and later identified to have autosomal recessive mutations in the *Phkg2* gene [1,34,35]. However, this rat model has not been studied in publication since 1996 [1]. Mice are a preferable model to rats as they are smaller in size, have a shorter gestation period, and generally cost less to maintain [36]. To date there are no established mouse models associated with liver GSD IX γ2 [26,27]. Here we identify the first mouse model for GSD IX γ2. Our laboratory has established the first successful breeding mouse colony to generate complete *Phkg2* knockout (*Phkg2*$^{-/-}$) mice. Results of this study provide evidence that the mouse model successfully recapitulates the liver-specific pathophysiology seen in GSD IX γ2 patients.

2. Methods

2.1. Generation of GSD IX γ2 Mice (Phkg2⁻/⁻)

Heterozygous *Phkg2* mutant (*Phkg2*$^{+/-}$) mice carrying the *Phkg2*$^{tm1.1}$ knockout allele (C57BL/6 N-*Phkg2*$^{tm1.1(KOMP)Vlcg}$/JMmucd, RRID:MMRRC_049060-UCD) were purchased from the Mutant Mouse Resource and Research Center (MMRRC) at University of California at Davis and then cross-bred to produce homozygous *Phkg2* knockout (KO, *Phkg2*$^{-/-}$) mice and wild-type (WT, *Phkg2*$^{+/+}$) controls. Pieces of tails were collected for genomic DNA extraction to confirm genotype by PCR. Primer pairs GGGAGCAGGGATTGCTACTG (Forward 1) and TTCCTCAGGGTTCCTGTTCTG (Reverse 1) were used for genotyping the KO allele and GGTAAACTGGCTCGGATTAGGG (Forward 2) and TTGACTGTAGCGGCTGATGTTG (Reverse 2) were used for the WT allele [37,38].

2.2. Fasting and Dissection of Mice

3 month old KO and WT mice were fasted for 24 h. Equal numbers of male and female mice were used between WT and KO groups. Apart from the body weight growth curve, all assays were performed specifically on samples from 3 month old mice. Blood and urine samples were collected. Mice were euthanized for tissue collection. After dissection, tissue was frozen on dry ice and stored at −80 °C for future biochemical assays or fixed in 10% neutral-buffered formalin (NBF) for 48 h for future histological analysis. All animal experiments were performed under approval of the Duke University Institutional Animal Care and Use Committee (IACUC) and under the guidelines from the National Institute of Health guide for the care and use of laboratory animals [39].

2.3. Measurement of Liver: Body Weight Ratio

Body weight was measured on a cohort of mice at 1 month, 2 months, and 3 months of age. These mice were not sacrificed. Body weight at 3 months of age was measured on a separate cohort of mice immediately followed by euthanasia, liver dissection, and liver weight measurement. Whole liver was collected and weighed to evaluate the ratio of liver weight to body weight. Liver weight was reported as a percent of body weight using the ratio of Liver weight/Body Weight (LW/BW) *100 as a metric for hepatomegaly.

2.4. RT-qPCR

RT-qPCR was performed to measure the transcription levels of the *Phkg2* gene. Equal weights of tissue were homogenized in cold lysis buffer [PBS containing 1% NP40, 0.5% sodium deoxycholate, 0.1% SDS and a protease/phosphatase inhibitor cocktail (Cell Signaling Technology, Danvers, MA)] using an electric homogenizer. Tissue lysates were cleared by centrifugation at 18,000g at 4 °C for 15 min. RNA isolation was performed on tissue lysates using the RNeasy mini kit (Qiagen) per manufacturer's instructions. The concentration and purity of RNA was assessed using NANODROP 2000 (Thermo Scientific). RNA was reverse transcribed into cDNA using the iScript cDNA Synthesis Kit (Bio-Rad Laboratories). RT-qPCR was performed using SYBR Green and the LightCycler 480 System (Roche, Basel, Switzerland) according to the manufacturer's instructions

with three technical replicates. *Phkg2* gene expression was measured relative to β-Actin. The following primers were used: *Phkg2* Forward 5'-GAGATGCACATTCTTCGCCA-3' *Phkg2* Reverse 5'-TCCTTTCCGCATCAGGTCAAA-3′ (Eton Bioscience), β-actin forward: 5'-AGATGTGGATCAGCAAGCAG –3′, β-Actin reverse: 5′-GCGCAAGTTAGGTTTTGTCA-3′ (Integrated DNA Technologies). The primers were designed to span different exons to ensure there was no amplification of genomic DNA. Relative gene expression compared to the housekeeping gene β-actin was calculated using the Delta-Delta Cycle Threshold (Ct) method [40].

2.5. PhK Enzymatic Activity

PhK enzyme activity was analyzed in frozen liver samples using standard spectrophotometric methods used by Glycogen Storage Disease Laboratory at DUHS. The assay is composed of three step reactions; the first step is set to activate the Phosphorylase b to Phosphorylase a. The second step involves breakdown of Glycogen in the presence of glycogen phosphorylase to release the free glucose molecule in the form of Glucose-1-phosphate. The last step uses Glucose reagent (Infinity™; Cat No. TR15421; ThermoScientific - Fisher Diagnostics, Middletown, VA, USA), which coverts Glucose-1-Phosphate to glucose-6-phosphate in the presence of Phosphoglucomutase. G-6-P is then oxidized and NAD+ is converted to NADH by G-6-P dehydrogenase. The amount of NADH formed is proportional to the concentration of glucose in the sample and is measured as absorbance at 340 nm. Enzyme activity was expressed as µmol/min/mg of liver tissue [15,41].

2.6. Glycogen Content Assay

Frozen tissues were homogenized in distilled water (1 mg of tissue/20 µL of water) using an electric homogenizer. Homogenization was followed by sonication for 15 s and centrifugation at 18,000g at 4 °C for 15 min. The 1:5 diluted lysates were boiled for 3 min to inactivate endogenous enzymes. Samples were incubated with 0.175 U/mL (final concentration in the reaction) of amyloglucosidase (Sigma-Aldrich Co., St. Louis, MO) for 90 min at 37 °C. The mixtures were boiled for 3 min to stop the reaction. 30 µL of the mixtures were incubated with 1 mL of Pointe Scientific Glucose Hexokinase Liquid Reagent (Fisher, Hampton, NH) for 10 min at room temperature. Absorbance was measured at 340 nm with a UV-VIS spectrophotometer (Shimadzu UV-1700 PharmaSpec) [42,43].

2.7. Histology

Fresh tissue samples were fixed in 10% NBF for 48 h and post-fixed with 1% periodic acid (PA) in 10% NBF for 48 h at 4 °C. Samples were washed with PBS, dehydrated with ascending grades of alcohol, cleared with xylene, and infiltrated with paraffin. Sections were cut with a microtome and mounted for staining.

For periodic acid-Schiff (PAS), slides were processed based on previously described methodology [42]. In brief, slides were deparaffinized and rehydrated. Slides were oxidized with freshly made 0.5% PA for 5 min and rinsed with distilled water for 1 min. Slides were then stained with Schiff reagent for 15 min and washed with tap water for 10 min. Slides were counterstained with Hematoxylin, rinsed with tap water, and incubated with bluing

reagent for 1 min. Slides were then dehydrated and mounted. The periodic acid oxidizes glycogen to an aldehyde product which reacts with Schiff reagent to produce a purple stain.

For Hematoxylin and Eosin staining (H&E), slides were treated based on previously described methodology [44]. In brief, slides were deparaffinized and rehydrated. Slides were stained with hematoxylin solution for 3 min, washed with running water and then stained with Eosin Y solution for 2 min. Slides were then dehydrated and mounted.

For Masson's Trichrome staining, slides were treated using the Sigma-Aldrich Masson's Trichrome Stain Kit No. HT15. Slides were deparaffinized and rehydrated. Slides were incubated in Bouin's solution at room temperature overnight. Slides were washed with running tap water, stained with Weigert's Iron Hematoxylin solution for 5 min, washed with running tap water, stained with Biebrich Scarlet-Acid Fuschin for 5 min, rinsed with distilled water, stained with phosphotungstic/phosphomolybdic Acid for 5 min, rinsed with distilled water, stained in Aniline Blue Solution for 5 min, rinsed with distilled water, stained in 1% acetic acid for 2 min, and rinsed in distilled water. Slides were then dehydrated and mounted. All imaging of slides was performed using a BZ-X710 microscope (Keyence America, Itasca, IL).

2.8. Blood & Urine Analyses

Blood was sampled at 3 months of age after 24 h of fasting via submandibular bleeding. Whole blood was sampled for blood glucose and ketones at hour intervals of fasting. Blood glucose levels were measured using the AlphaTRAK2 whole blood glucometer and blood ketone levels were measured using the Nova Max Glucose Ketone Meter [45]. Additional blood was collected in a red top collection tube and centrifuged at 2000g, 4 °C for 10 min to isolate serum. Serum samples were sent out for liver and lipid panel testing by a commercial laboratory (IDEXX Laboratories, Inc.). The liver panel included alkaline phosphatase (ALP), aspartate aminotransferase (AST), alanine aminotransferase (ALT), conjugated bilirubin (CB), unconjugated bilirubin (UCB), total bilirubin (TB), creatine kinase (CK), total protein (TP), albumin (ALB), and gamma-glutamyl transferase (GGT). The lipid panel included total cholesterol (TC), triglycerides, low-density lipoprotein (LDL), and high-density lipoprotein (HDL). Urine samples were collected at 3 months of age after 24 h of fasting. Individual mice were restrained over a collection device. Gentle pressure was placed on the belly to stimulate urination. Per mouse, 50 μL of urine was collected in individual 1.7 mL Eppendorf tubes. Samples were shipped on dry ice to the Duke University Health System Biochemical Genetics Laboratory for urine glucose tetrasaccharide Glcα1–6Glcα1–4Glcα1–4Glc (Glc$_4$) analysis, also referred to as hexose tetrasaccharide (Hex$_4$), based on the laboratory's previously described mass spectrometry methods [46,47].

2.9. Statistical Analysis

All numerical data was evaluated using Prism software version 8 (GraphPad, La Jolla, CA). Statistical analysis of all quantitative data collected was performed using parametric unpaired t-tests to determine the differences between assays in male and female KO and WT groups. One star * indicated p value < 0.05. Two stars ** indicated $p < 0.01$. Three stars ***

indicated $p < 0.001$. Four stars **** indicated $p < 0.0001$. P value < 0.05 was considered a statistically significant difference.

3.   Results

3.1.   Generation of *Phkg2*–/– Mouse Model Verified at DNA Level

The *Phkg2tm1* knockout allele was generated with a targeting vector by replacing the entire PhK coding regions in the *Phkg2* allele with a DNA fragment containing the lacZ and LoxP-floxed neomycin expression cassettes (not shown). The *Phkg2tm1.1* knockout allele was generated via Cre-mediated excision of the neomycin selection cassette from the parental *Phkg2tm1* knockout allele (Fig. 1A). Genotype was confirmed via genomic DNA extraction, PCR, and gel electrophoresis. The first PCR product at 210 bp in length was amplified from the KO allele using the F1 and R1 primers. The second PCR product at 136 bp in length was amplified via PCR from the WT allele using the F2 and R2 primers. Heterozygous mice (HT) demonstrated both the KO and WT PCR products (Fig. 1B).

3.2.   Generation of *Phkg2*–/– Mouse Model Verified at RNA and Enzyme Level

RT-qPCR was performed with liver lysates from KO mice and WT controls. Primers were designed to identify levels of transcription for the *Phkg2* gene, with β-actin as a control. Transcription of the *Phkg2* gene was significantly decreased ($p < 0.001$) in KO mice compared to WT controls (Fig. 1C). PhK enzyme activity was also performed with liver lysates and was significantly decreased ($p < 0.0001$) in KO mice compared to WT controls. 6 KO (3 male, 3 female) 6 WT (3 male, 3 female) (Fig. 1D).

3.3.   Morphological Measurements in *Phkg2*–/– Mice Reveal Hepatomegaly

Total body weight was measured and compared for WT and KO mice at 1, 2, and 3 months of age. KO mice demonstrate significantly lower ($p < 0.001$) average body weight at 1 month of age. 20 WT (13 female, 7 male), 20 KO (13 female, 7 male). KO and WT mice demonstrated similar weights by 2 months of age. 2 months - 14 WT (7 male, 7 female), 14 KO (7 male, 7 female) and 3 months - 14 WT (7 male, 7 female), 14 KO (7 male, 7 female). (Fig. 2A). Liver weight (LW) was normalized to overall body weight (BW) as a quantitative metric for enlarged liver or hepatomegaly. % Liver weight (LW/BW*100) was significantly higher in KO mice when compared to WT controls. 17 WT (7 male, 10 female), 17 KO (7 male, 10 female; $p < 0.0001$) (Fig. 2B).

3.4.   Liver Glycogen Content is Significantly Elevated in *Phkg2*–/– Mice

There was a marked difference in PAS stain between KO and WT controls specific to the liver (Fig. 3A). For histology slides of brain, quadricep, kidney, and heart, there was minimal difference in the PAS stain between KO and WT controls 6 WT (3 male, 3 female), 6 KO (2 male, 4 female; Fig. 3A). The remarkable increase in PAS stain in the liver of KO mice was verified with glycogen content assay. Glycogen content in the liver was significantly elevated in KO mice compared with WT controls. 6 WT (3 male, 3 female), 6 KO (3 male, 3 female; $p < 0.0001$; Fig. 3B). Glycogen content assay confirmed that there was a significant difference in glycogen accumulation specific to the liver of KO mice, a key characteristic of liver GSD IX γ2.

3.5. *Phkg2$^{-/-}$* Mice Demonstrated Characteristic GSD Hepatocyte Architectural Changes and Early Perisinusoidal Fibrosis

On H&E stain, KO hepatocytes were heterogeneously enlarged with pale cytoplasm and distinct cell membranes, secondary to persistent glycogen accumulation. Nuclei were concentrated, pyknotic, and lateralized (Fig. 4A). Based on pathologist review, hepatocyte architectural changes were identified in 5 KO mice and 0 WT controls. 6 WT (4 male, 2 female), 5 KO (2 male, 3 female). These hepatocyte architectural changes are characteristic of the changes seen in patients with liver GSDs [48]. On Masson's Trichrome stain, KO mice showed evidence of early perisinusoidal liver fibrosis (Fig. 4B). Based on pathologist review, early perisinusoidal fibrosis was identified in 3 KO mice and 0 WT controls. 6 WT (4 male, 2 female), 8 KO (5 male, 3 female). Progressive liver fibrosis is characteristic in patients with liver GSDs [48,49].

3.6. *Phkg2$^{-/-}$* Mice Demonstrated Significant Increase in Serum AST, ALT, and Urine Hex$_4$

To create fasting blood glucose and ketone curves, KO and WT mice were fasted and measured for blood glucose and ketones. When compared to WT controls, KO mice demonstrated significant hypoglycemia for 0 and 8 h of fasting. During the period of hypoglycemia, while blood ketones did increase in both groups, there was not a significant difference in blood ketones between KO mice and WT controls. 10 WT (5 male, 5 female) and 10 KO (5 male, 5 female; Fig. 5A,B). Urine samples were evaluated for Hex$_4$, a known biomarker of glycogen accumulation. In line with the elevated glycogen accumulation seen on PAS stain and glycogen assay (Fig. 4), there was a significant elevation in urine Hex$_4$ in KO mice compared to WT controls. 6 WT (3 male, 3 female), 6 KO (3 male, 3 female) ($p < 0.01$; Fig. 5C). Serum samples were collected for liver and lipid panel analyses. Liver enzymes including ALT and AST were significantly elevated in KO mice vs. WT controls. 5 WT (2 male, 3 female), 5 KO (2 male, 3 female) (ALT $p < 0.0001$, AST $p < 0.0001$; Fig. 5D, E). No significant differences were observed for GGT, TP, Albumin, TB, CB, UCB, TC, triglycerides, LDL, and HDL.

4. Discussion

Patients with liver GSD IX generally present with liver-specific symptoms including hepatomegaly, hypoglycemia, growth delay, and elevated liver blood markers. For patients with GSD IX γ2, symptoms persist and progress to severe liver disease [2,12,[16], [17], [18], [19],21]. As exemplified in the literature, 95.8% of published case reports for GSD IX γ2 patients who received a liver biopsy reported features of liver fibrosis and/or cirrhosis [14]. Severe liver pathology places individuals with GSD IX γ2 at high risk for developing progressive liver disease, advancing from liver fibrosis, cirrhosis, to liver failure, hepatocellular carcinoma and death. Despite the life-threatening phenotype of GSD IX γ2, research regarding the disease and definitive treatment options has been minimal to date [14]. Here we have identified the first mouse model for GSD IX γ2, and provided evidence that the mouse model recapitulates the liver-specific disease phenotype seen in patients [48,49].

In the $Phkg2^{-/-}$ mouse, our data verified the loss of the $Phkg2$ gene at the DNA, RNA, and enzyme level. At the DNA level, genotyping confirmed that targeted deletion was achieved via insertion of the Velocigene-Regeneron targeted vector into exon 2 of the $Phkg2$ allele (Fig. 1A,B). At the RNA level, transcription of $Phkg2$ is virtually undetectable ($p < 0.001$) in KO mice compared to WT controls (Fig. 1C). At the enzyme level, PhK activity was significantly decreased ($p < 0.0001$) in KO mice when compared with WT controls (Fig. 1D). This decrease in PhK enzyme activity prevents adequate breakdown of glycogen into glucose, which leads to glycogen accumulation in the liver, the disease defining phenotype of GSD IX γ2. As seen in other glycogen storage disease models, a decrease in enzyme activity in one enzyme can have upstream or downstream effects on subsequent enzymes in the glycogen metabolism pathways [50,51]. Future research should include analysis of all enzymes in the glycogen metabolism pathways in our GSD IX γ2 mouse model. A better understanding of how glycogenolysis and glycogenesis enzyme expression and activity are altered in the GSD IX γ2 mouse model may inform metabolic reprogramming as a potential treatment.

As previously stated, patients with GSD IX generally present with liver-specific symptoms secondary to persistent liver glycogen accumulation. PAS-stained histology slides identified remarkable glycogen accumulation specific to the liver (Fig. 3A), which was confirmed by glycogen content analysis ($p < 0.0001$; Fig. 3B). In the $Phkg2^{-/-}$ mouse, KO mice demonstrated significant hepatomegaly secondary to glycogen accumulation, when compared to WT controls ($p < 0.0001$; Fig. 2B). The $Phkg2^{-/-}$ mouse also demonstrated liver glycogen-associated changes in blood and urine biomarkers. A serum liver panel demonstrated significantly elevated ALT and AST levels (Fig. 5D, E). Urine analysis demonstrated significantly elevated Hex_4 levels (Fig. 5C). When further stratified by sex, all significant data remained statistically significant (Figs. S1–S3). This is the first time that elevated Hex_4 levels, also known as Glc_4, have been associated with liver-only glycogen accumulation in an animal model. Glc_4 has been identified as a robust biomarker in muscle associated glycogen storage diseases such as Pompe (GSD II) [52]. In GSD III, Glc_4 can be elevated secondary to glycogen accumulation in liver and/or muscle [53]. Here we present the novel finding of elevated Glc_4 in the $Phkg2^{-/-}$ mouse, supporting the use of urine Glc_4 as a biomarker for liver-specific GSDs. Future work will require analysis of blood and urine biomarkers over different time points. With comparison to age matched histology, the analysis of blood and urine biomarkers at later ages will help us better understand liver disease progression with noninvasive tools. Histology slides from our mouse model mirror the architectural and fibrotic changes seen in GSD IX γ2 patients [48,49]. H&E-stained liver histology slides from liver GSD IX γ2 patients display hepatocytes that are heterogeneously enlarged with distinct cell membranes, pale cytoplasm, and concentrated, pyknotic, and lateralized nuclei. The pale cytoplasm identifies persistent glycogen accumulation. Based on board certified hepatobiliary pathologist review, all H&E-stained liver histology slides from our KO mice demonstrated these characteristic H&E hepatocyte changes (Fig. 4A). Masson's Trichrome stained histology slides from 3 of our KO mice demonstrated early perisinusoidal liver fibrosis, a sign of early liver damage (Fig. 4B). Trichrome stained histology slides from liver GSD patients similarly display progressive liver fibrosis [14]. Changes are also visible at lower magnification (Fig. S4). Identification of initial liver

structural damages allows for the description of further liver disease progression. Based on the lessons learned from previously described liver GSD patients, we know that liver damage/fibrosis becomes gradually more progressive and severe in patients with age. Based on our published laboratory work, we also know that severe liver fibrosis can be captured in GSD mouse models [42,43,[54], [55], [56]]. Future work will require longitudinal evaluation. The analysis of Trichrome stained histology slides at later ages will allow us to capture the progressive stages of liver fibrosis in our mouse model and compare these changes to the progressive liver disease seen in patients with GSD IX γ2.

In conclusion, our laboratory has characterized the first mouse model for liver GSD IX γ2 and demonstrated that the model recapitulates the liver-specific glycogen accumulation phenotype of patients with GSD IX γ2. Future research is needed to characterize the mouse model at later ages, which will better our understanding of liver GSD IX γ2 disease progression. The *Phkg2*$^{-/-}$ mouse will provide the first platform for the design and examination of novel, long term, definitive liver GSD IX γ2 therapeutics.

Supplementary Material

Refer to Web version on PubMed Central for supplementary material.

Acknowledgements

9. REFERENCES

[1]. Maichele AJ, Burwinkel B, Maire I, Søvik O, Kilimann MW, Mutations in the testis/liver isoform of the phosphorylase kinase γ subunit (PHKG2) cause autosomal liver glycogenosis in the gsd rat and in humans, Nat. Genet 14 (1996) 337–340. 10.1038/ng1196-337. [PubMed: 8896567]

[2]. Kishnani PS, Goldstein J, Austin SL, Arn P, Bachrach B, Bali DS, Chung WK, El-Gharbawy A, Brown LM, Kahler S, Pendyal S, Ross KM, Tsilianidis L, Weinstein DA, Watson MS, Diagnosis and management of glycogen storage diseases type VI and IX: a clinical practice resource of the American College of Medical Genetics and Genomics (ACMG), Genet. Med 21 (2019) 772–789. 10.1038/s41436-018-0364-2. [PubMed: 30659246]

[3]. Brushia RJ, Walsh DA, Phosphorylase Kinase: The Complexity of its Regulation is Reflected in the complexity of its Structure, Front. Biosci 4 (1999) 618–641. 10.2741/brushia.

[4]. Vénien-Bryan C, Jonic S, Skamnaki V, Brown N, Bischler N, Oikonomakos N, Boisset N, Johnson LN, The Structure of Phosphorylase Kinase Holoenzyme at 9.9 Å Resolution and Location of the Catalytic Subunit and the Substrate Glycogen Phosphorylase, Structure. 17 (2009) 117–127. 10.1016/j.str.2008.10.013. [PubMed: 19141288]

[5]. Skamnaki VT, Owen DJ, Noble MEM, Lowe ED, Lowe G, Oikonomakos NG, Johnson LN, Catalytic Mechanism of Phosphorylase Kinase Probed by Mutational Studies, Biochemistry. 38 (1999) 14718–14730. 10.1021/bi991454f. [PubMed: 10545198]

[6]. Lowe ED, Noble MEM, Skamnaki VT, Oikonomakos NG, Owen DJ, Johnson LN, The crystal structure of a phosphorylase kinase peptide substrate complex: kinase substrate recognition, EMBO J. 16 (1997) 6646–6658. 10.1093/emboj/16.22.6646. [PubMed: 9362479]

[7]. Owen DJ, Noble M, Garman EF, Papageorigiou AC, Johnson LN, Two structures of the catalytic domain of phosphorylase kinase: an active protein kinase complexed with substrate analogue and product, Structure. 3 (1995) 467–482. 10.1016/S0969-2126(01)00180-0. [PubMed: 7663944]

[8]. Newgard CB, Hwang PK, Fletterick RJ, The family of glycogen phosphorylases: structure and function, Crit. Rev. Biochem. Mol. Biol 24 (1989) 69–99. 10.3109/10409238909082552. [PubMed: 2667896]

[9]. Willems PJ, Gerver WJM, Berger R, Fernandes J, The natural history of liver glycogenosis due to phosphorylase kinase deficiency: A longitudinal study of 41 patients, Eur. J. Pediatr 149 (1990) 268–271. 10.1007/BF02106291. [PubMed: 2303074]

[10]. Li C, Huang L, Tian L, Chen J, Li S, Yang Z, PHKG2 mutation spectrum in glycogen storage disease type IXc: A case report and review of the literature, J. Pediatr. Endocrinol. Metab 31 (2018) 331–338. 10.1515/jpem-2017-0170. [PubMed: 29360628]

[11]. Roscher A, Patel J, Hewson S, Nagy L, Feigenbaum A, Kronick J, Raiman J, Schulze A, Siriwardena K, Mercimek-Mahmutoglu S, The natural history of glycogen storage disease types VI and IX: Long-term outcome from the largest metabolic center in Canada, Mol. Genet. Metab 113 (2014) 171–176. 10.1016/j.ymgme.2014.09.005. [PubMed: 25266922]

[12]. Herbert M, Goldstein JL, Rehder C, Austin S, Kishnani PS, Bali DS, Phosphorylase Kinase Deficiency, GeneReviews. (2011). https://www.ncbi.nlm.nih.gov/books/NBK55061/ (accessed March 14, 2020).

[13]. Wolfsdorf JI, Holm IA, Weinstein DA, Glycogen storage diseases: Phenotypic, genetic, and biochemical characteristics, and therapy, Endocrinol. Metab. Clin. North Am 28 (1999) 801–823. 10.1016/S0889-8529(05)70103-1. [PubMed: 10609121]

[14]. Fernandes SA, Cooper GE, Gibson RA, Kishnani PS, Benign or not benign? Deep phenotyping of liver Glycogen Storage Disease IX, Mol. Genet. Metab (2020). 10.1016/j.ymgme.2020.10.004.

[15]. Bali DS, Goldstein JL, Fredrickson K, Rehder C, Boney A, Austin S, Weinstein DA, Lutz R, Boneh A, Kishnani PS, Variability of disease spectrum in children with liver phosphorylase kinase deficiency caused by mutations in the PHKG2 gene, Mol. Genet. Metab 111 (2014) 309–313. 10.1016/j.ymgme.2013.12.008. [PubMed: 24389071]

[16]. Burwinkel B, Shiomi S, Al Zaben A, Kilimann MW, Liver glycogenosis due to phosphorylase kinase deficiency: PHKG2 gene structure and mutations associated with cirrhosis, Hum. Mol. Genet 7 (1998) 149–154. 10.1093/hmg/7.1.149. [PubMed: 9384616]

[17]. Burwinkel B, Tanner MS, Kilimann MW, Phosphorylase kinase deficient liver glycogenosis: progression to cirrhosis in infancy associated with PHKG2 mutations (H144Y and L225R), J. Med. Genet 37 (2000) 376–7. 10.1136/jmg.37.5.376. [PubMed: 10905889]

[18]. Søvik O, de Barsy T, Maehle B, Phosphorylase kinase deficiency: Severe glycogen storage disease with evidence of autosomal recessive mode of inheritance, Eur. J. Pediatr 139 (1982) 210. 10.1007/BF01377363. [PubMed: 6962066]

[19]. Albash B, Imtiaz F, Al-Zaidan H, Al-Manea H, Banemai M, Allam R, Al-Suheel A, Al-Owain M, Novel PHKG2 mutation causing GSD IX with prominent liver disease: Report of three cases and review of literature, Eur. J. Pediatr 173 (2014) 647–653. 10.1007/s00431-013-2223-0. [PubMed: 24326380]

[20]. Van Beurden EACM, De Graaf M, Wendel U, Gitzelmann R, Berger R, Van Den Berg IET, Autosomal recessive liver phosphorylase kinase deficiency caused by a novel splice-site mutation in the gene encoding the liver gamma subunit (PHKG2), Biochem. Biophys. Res. Commun 236 (1997) 544–548. 10.1006/bbrc.1997.7006. [PubMed: 9245685]

[21]. Beauchamp NJ, Dalton A, Ramaswami U, Niinikoski H, Mention K, Kenny P, Kolho KL, Raiman J, Walter J, Treacy E, Tanner S, Sharrard M, Glycogen storage disease type IX: High variability in clinical phenotype, Mol. Genet. Metab 92 (2007) 88–99. 10.1016/j.ymgme.2007.06.007. [PubMed: 17689125]

[22]. Rawal N, Yazigi N, Pediatric Liver Transplantation, Pediatr. Clin. North Am 64 (2017) 677–684. 10.1016/j.pcl.2017.02.003. [PubMed: 28502445]

[23]. Guénet JL, Animal models of human genetic diseases: do they need to be faithful to be useful?, Mol. Genet. Genomic Med 286 (2011) 1–20. 10.1007/s00438-011-0627-y.

[24]. Smithies O, Animal models of human genetic diseases, Trends Genet. 9 (1993) 112–116. 10.1016/0168-9525(93)90204-U. [PubMed: 8516844]

[25]. Wine JJ, Dean M, Glavac D, Natural animal models of human genetic diseases., Methods Mol. Med 70 (2002) 31–46. 10.1385/1-59259-187-6:31.

[26]. Walvoort HC, Glycogen Storage Diseases in Animals and Their Potential Value as Models of Human Disease, 1983.

[27]. Akman HO, Raghavan A, Craigen WJ, Animal models of glycogen storage disorders, Prog. Mol. Biol. Transl. Sci 100 (2011) 369–388. 10.1016/B978-0-12384878-9.00009-1. [PubMed: 21377631]

[28]. Gross SR, Mayer SE, Longshore MA, Stimulation of Glycogenolysis by Beta Adrenergic Agonists in Skeletal Muscle of Mice with the Phosphorylase Kinase Deficiency Mutation (I strain), J. Pharmacol. Exp. Ther 198 (1976).

[29]. Mefford AM, Ayers CC, Rowland NS, Rice NA, The PHKA1 deficient I/LnJ mouse exhibits endurance exercise deficiency with no compensatory changes in glycolytic gene expression, Open J. Mol. Integr. Physiol 03 (2013) 87–94. 10.4236/ojmip.2013.32014.

[30]. Varsanyi M, Grosxhel-Stewart U, Heilmeyer LM, Characterization of a Ca2+-Dependent Protein Kinase in Skeletal Muscle Membranes of I-Strain and Wild-Type Mice, Eur. J. Biochem 87 (1978) 331–340. 10.1111/j.1432-1033.1978.tb12382.x. [PubMed: 668698]

[31]. Lyon JB, Porter J, The Relation of Phosphosylase to Glycogenolysis in Skeletal Muscle and Heart of Mice, J. Biol. Chem 238 (1963) 1–12. [PubMed: 13931951]

[32]. Varsfinyi M, Vrbica A, Heiimeyer LMG, X-Linked Dominant Inheritance of Partial Phosphorylase Kinase Deficiency in Mice, Biochem. Genet 18 (1980) 247–261. 10.1007/BF00484240. [PubMed: 7447922]

[33]. Wilson LH, Estrella A, Weinstein DA, Lee YM, Effects of PhK Deficiency in a Mouse Model of Glycogen Storage Disease Type IX, in: Am. Soc. Gene Cell Ther, American Society of Gene and Cell Therapy, 2018.

[34]. Malthus R, Clark DG, Watts C, Sneyd JGT, Glycogen-storage disease in rats, a genetically determined deficiency of liver phosphorylase kinase, Biochem. J 188 (1980) 99–106. 10.1042/bj1880099. [PubMed: 6931596]

[35]. Haynes D, Hall P, Clark D, A Glycogen Storage Disease in Rats, Cell Pathol. 42 (1983) 289–301. 10.1007/BF02890391.

[36]. Bryda EC, The Mighty Mouse: the impact of rodents on advances in biomedical research, Mo. Med 110 (2013) 207–211. [PubMed: 23829104]

[37]. Valenzuela DM, Murphy AJ, Frendewey D, Gale NW, Economides AN, Auerbach W, Poueymirou WT, Adams NC, Rojas J, Yasenchak J, Chernomorsky R, Boucher M, Elsasser AL, Esau L, Zheng J, Griffiths JA, Wang X, Su H, Xue Y, Dominguez MG, Noguera I, Torres R, Macdonald LE, Stewart AF, DeChiara TM, Yancopoulos GD, High-throughput engineering of the mouse genome coupled with high-resolution expression analysis, Nat. Biotechnol 21 (2003) 652–659. 10.1038/nbt822. [PubMed: 12730667]

[38]. Dickinson ME, Flenniken AM, Ji X, Teboul L, Wong MD, White JK, Meehan TF, Weninger WJ, Westerberg H, Adissu H, Baker CN, Bower L, Brown JM, Brianna Caddle L, Chiani F, Clary D, Cleak J, Daly MJ, Denegre JM, Doe B, Dolan ME, Edie SM, Fuchs H, Gailus-Durner V, Galli A, Gambadoro A, Gallegos J, Guo S, Horner NR, wei Hsu C, Johnson SJ, Kalaga S, Keith LC, Lanoue L, Lawson TN, Lek M, Mark M, Marschall S, Mason J, McElwee ML, Newbigging S, Nutter LMJ, Peterson KA, Ramirez-Solis R, Rowland DJ, Ryder E, Samocha KE, Seavitt JR, Selloum M, Szoke-Kovacs Z, Tamura M, Trainor AG, Tudose I, Wakana S, Warren J, Wendling O, West DB, Wong L, Yoshiki A, MacArthur DG, Tocchini-Valentini GP, Gao X, Flicek P, Bradley A, Skarnes WC, Justice MJ, Parkinson HE, Moore M, Wells S, Braun RE, Svenson KL, Hrabe de Angelis M, Herault Y, Mohun T, Mallon AM, Mark Henkelman R, Brown SDM, Adams DJ, Kent Lloyd KC, McKerlie C, Beaudet AL, Bucan M, Murray SA, McKay M, Urban B, Lund C, Froeter E, LaCasse T, Mehalow A, Gordon E, Donahue LR, Taft R, Kutney P, Dion S, Goodwin L, Kales S, Urban R, Palmer K, Pertuy F, Bitz D, Weber B, Goetz-Reiner P, Jacobs H, Le Marchand E, El Amri A, El Fertak L, Ennah H, Ali-Hadji D, Ayadi A, Wattenhofer-Donze M, Jacquot S, André P, Birling MC, Pavlovic G, Sorg T, Morse I, Benso F, Stewart ME, Copley C, Harrison J, Joynson S, Guo R, Qu D, Spring S, Yu L, Ellegood J, Morikawa L, Shang X, Feugas

P, Creighton A, Penton PC, Danisment O, Griggs N, Tudor CL, Green AL, Icoresi Mazzeo C, Siragher E, Lillistone C, Tuck E, Gleeson D, Sethi D, Bayzetinova T, Burvill J, Habib B, Weavers L, Maswood R, Miklejewska E, Woods M, Grau E, Newman S, Sinclair C, Brown E, Ayabe S, Iwama M, Murakami A, High-throughput discovery of novel developmental phenotypes, Nature. 537 (2016) 508–514. 10.1038/nature19356. [PubMed: 27626380]

[39]. Garber JC, Barbee RW, Bielitzki JT, Clayton LA, Donovan JC, Hendriksen CFM, Kohn DF, Lipman NS, Locke PA, Melcher J, Quimby FW, Turner PV, Wood GA, Würbel H, Guide for the care and use of laboratory animals, 2011.

[40]. Livak KJ, Schmittgen TD, Analysis of relative gene expression data using real-time quantitative PCR and the 2- CT method, Methods. 25 (2001) 402–408. 10.1006/meth.2001.1262. [PubMed: 11846609]

[41]. Tuchman M, Brown BI, Burke BA, Ulstrom RA, Clinical and laboratory observations in a child with hepatic phosphorylase kinase deficiency, Metabolism. 35 (1986) 627–633. 10.1016/0026-0495(86)90169-1. [PubMed: 3459948]

[42]. Lim JA, Yi H, Gao F, Raben N, Kishnani PS, Sun B, Intravenous Injection of an AAV-PHP.B Vector Encoding Human Acid α-Glucosidase Rescues Both Muscle and CNS Defects in Murine Pompe Disease, Mol. Ther. - Methods Clin. Dev 12 (2019) 233–245. 10.1016/j.omtm.2019.01.006. [PubMed: 30809555]

[43]. Lim B, J A, Choi SJ, Gao F, Kishnani P. and Sun, Correction of Glycogen Storage Disease Type III with an AAV Vector Encoding a Bacterial Glycogen Debranching Enzyme, Mol. Ther 27 (2019) 17–17. 10.1016/j.omtm.2020.05.034. [PubMed: 30527757]

[44]. Cardiff RD, Miller CH, Munn RJ, Manual hematoxylin and eosin staining of mouse tissue sections, Cold Spring Harb. Protoc 2014 (2014) 655–658. 10.1101/pdb.prot073411. [PubMed: 24890205]

[45]. Ayala JE, Samuel VT, Morton GJ, Obici S, Croniger CM, Shulman GI, Wasserman DH, McGuinness OP, Standard operating procedures for describing and performing metabolic tests of glucose homeostasis in mice, DMM Dis. Model. Mech 3 (2010) 525–534. 10.1242/dmm.006239. [PubMed: 20713647]

[46]. Young SP, Khan A, Stefanescu E, Seifts AM, Hijazi G, Austin S, Kishnani PS, Diurnal variability of glucose tetrasaccharide (Glc 4) excretion in patients with glycogen storage disease type III, JIMD Rep. (2020) jmd2.12181. 10.1002/jmd2.12181.

[47]. Young SP, Stevens RD, An Y, Chen YT, Millington DS, Analysis of a glucose tetrasaccharide elevated in Pompe disease by stable isotope dilution-electrospray ionization tandem mass spectrometry, Anal. Biochem 316 (2003) 175–180. 10.1016/S0003-2697(03)00056-3. [PubMed: 12711338]

[48]. Halaby CA, Young SP, Austin S, Stefanescu E, Bali D, Clinton LK, Smith B, Pendyal S, Upadia J, Schooler GR, Mavis AM, Kishnani PS, Liver fibrosis during clinical ascertainment of glycogen storage disease type III: a need for improved and systematic monitoring, Genet. Med 21 (2019) 2686–2694. 10.1038/s41436-019-0561-7. [PubMed: 31263214]

[49]. Degrassi I, Deheragoda M, Creegen D, Mundy H, Mustafa A, Vara R, Hadzic N, Liver histology in children with glycogen storage disorders type VI and IX, Dig. Liver Dis (2020). 10.1016/j.dld.2020.04.017.

[50]. Yi H, Brooks ED, Thurberg BL, Fyfe JC, Kishnani PS, Sun B, Correction of glycogen storage disease type III with rapamycin in a canine model, (n.d.). 10.1007/s00109-014-1127-4.

[51]. Taylor KM, Meyers E, Phipps M, Kishnani PS, Cheng SH, Scheule RK, Moreland RJ, Dysregulation of Multiple Facets of Glycogen Metabolism in a Murine Model of Pompe Disease, PLoS One. 8 (2013) e56181. 10.1371/journal.pone.0056181.

[52]. Kishnani PS, Steiner RD, Bali D, Berger K, Byrne BJ, Case L, Crowley JF, Downs S, Howell RR, Kravitz RM, Mackey J, Marsden D, Martins AM, Millington DS, Nicolino M, O'Grady G, Patterson MC, Rapoport DM, Slonim A, Spencer CT, Tifft CJ, Watson MS, Pompe disease diagnosis and management guideline, Genet. Med 8 (2006) 267–288. 10.1097/01.gim.0000218152.87434.f3. [PubMed: 16702877]

[53]. Kishnani PS, Austin SL, Arn P, Bali DS, Boney A, Case LE, Chung WK, Desai DM, El-Gharbawy A, Haller R, Smit GPA, Smith AD, Hobson-Webb LD, Wechsler SB, Weinstein DA,

Watson MS, Glycogen Storage Disease Type III diagnosis and management guidelines, Genet. Med 12 (2010) 446–463. 10.1097/GIM.0b013e3181e655b6. [PubMed: 20631546]

[54]. Liu KM, Wu JY, Chen YT, Mouse model of glycogen storage disease type III, Mol. Genet. Metab 111 (2014) 467–476. 10.1016/j.ymgme.2014.02.005. [PubMed: 24613482]

[55]. Akman HO, Sheiko T, Tay SKH, Finegold MJ, DiMauro S, Craigen WJ, Generation of a novel mouse model that recapitulates early and adult onset glycogenosis type IV, Hum. Mol. Genet 20 (2011) 4430–4439. 10.1093/hmg/ddr371. [PubMed: 21856731]

[56]. Wilson LH, Cho J, Estrella A, Smyth JA, Wu R, Chengsupanimit T, Brown LM, Weinstein DA, Lee YM, Liver Glycogen Phosphorylase Deficiency Leads to Profibrogenic Phenotype in a Murine Model of Glycogen Storage Disease Type VI, Hepatol. Commun 3 (2019) 1544–1555. 10.1002/hep4.1426. [PubMed: 31701076]
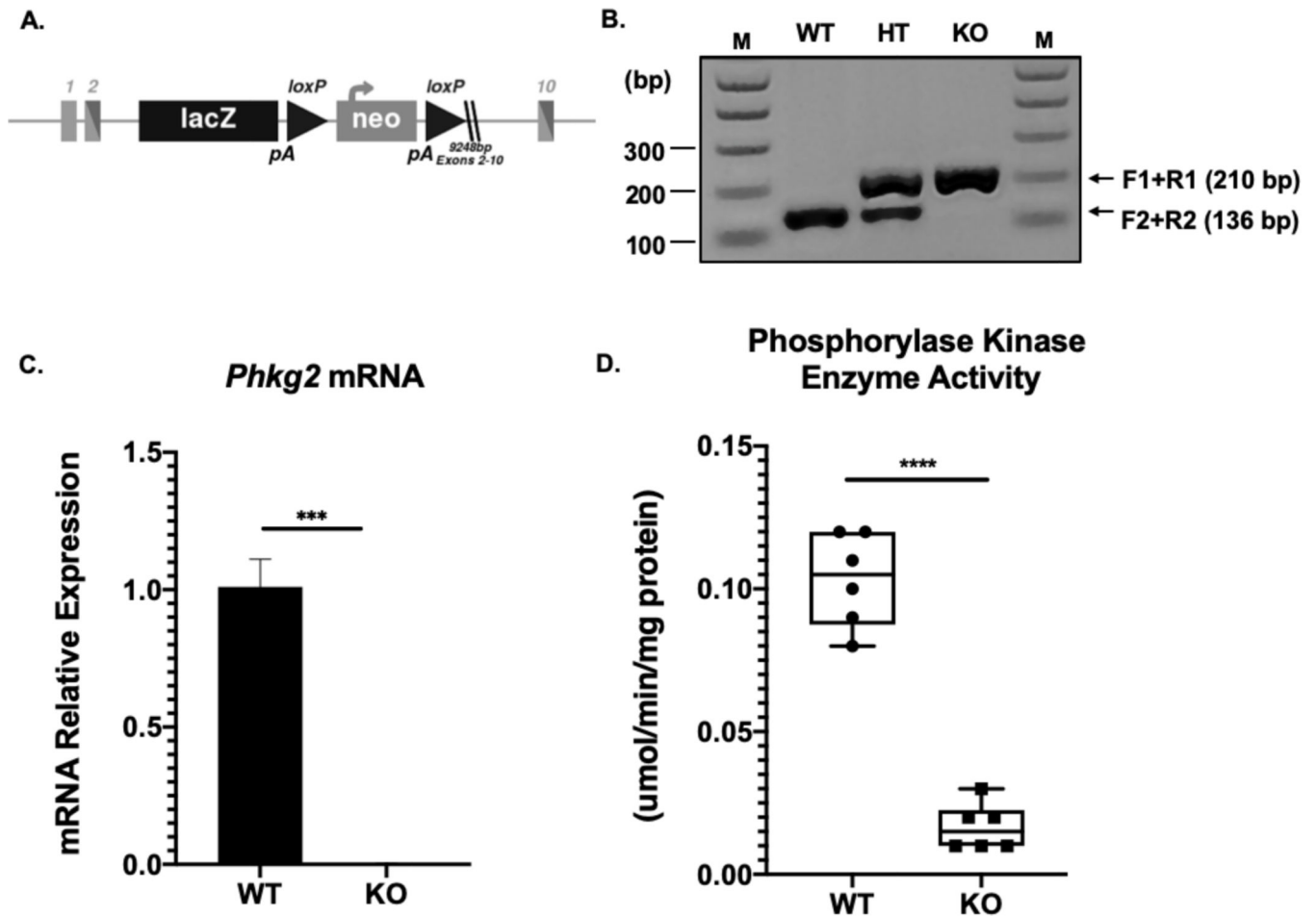
Figure 1 –. Generation of *Phkg2*^{−/−} mouse model verified at DNA, mRNA, and enzyme activity level. *(A) Illustration of the Phkg2*^{tm1.1} *knockout allele*.
Targeted deletion of the critical exons containing the entire PhK protein coding regions was achieved via a non-conditional knockout approach followed by Cre-mediated excision of the neomycin selection cassette. *(B) Genotyping by PCR*. F1, R1 primers added to genomic DNA of knockout (KO) mice generate a PCR fragment at 210 bp in length. F2, R2 primers added to genomic DNA of wild type (WT) mice generate a PCR fragment at 136 bp in length. Primers added to genomic DNA of Heterozygous (HT) mice generate both PCR fragments. M indicates the size marker. *(C) Phkg2 mRNA*. RT-qPCR was performed to assess transcription of the *Phkg2* gene. b-actin served as the loading control. The level of transcription was significantly higher in KO mice than WT controls. KO n=3, WT n=3. ***p<0.001. *(D) PhK Enzyme Activity*. Enzyme activity was assayed with liver lysates from KO mice and WT controls. Phosphorylase kinase (PhK) activity was significantly less in KO mice compared to WT controls. 6 WT (3 male, 3 female), 6 KO (3 male, 3 female). ****p<0.0001.
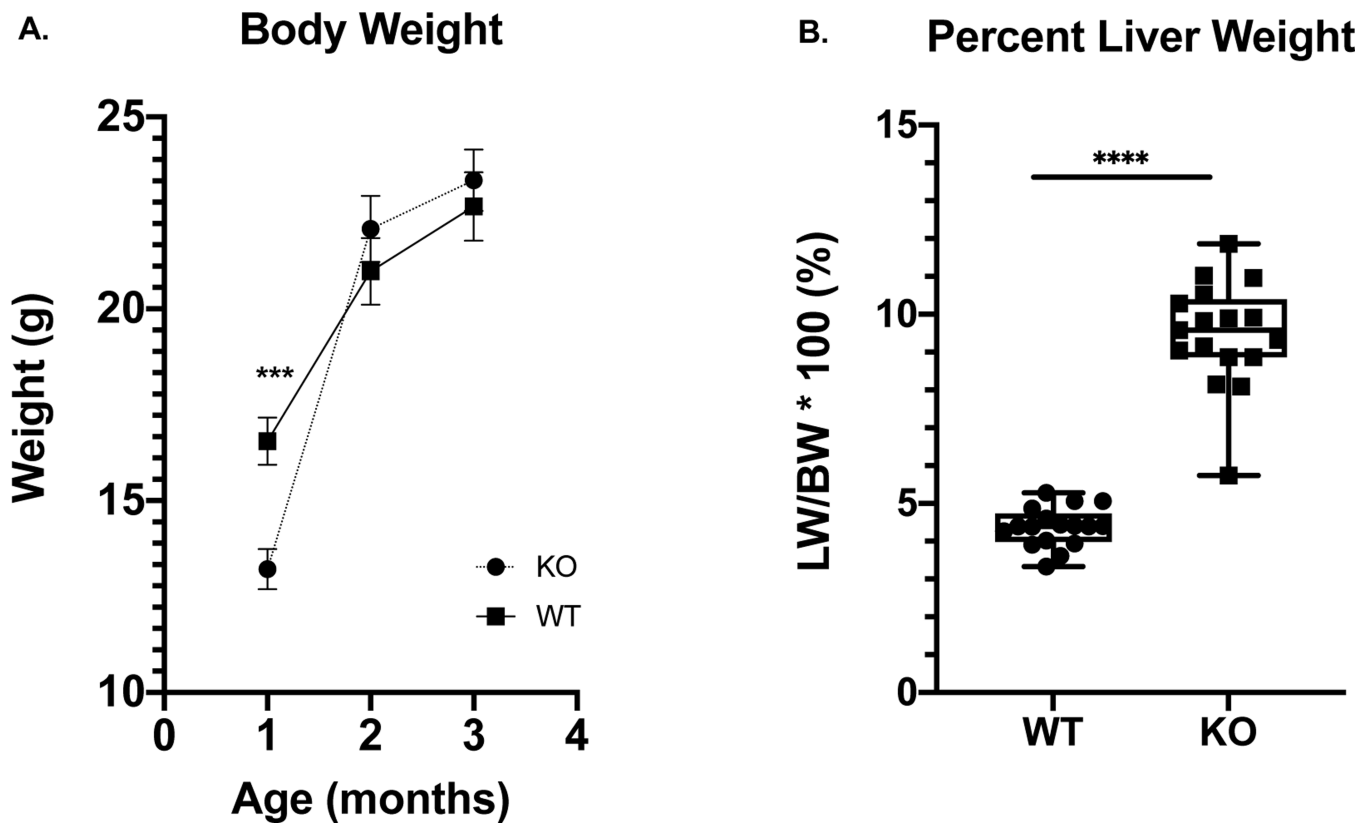
A. Body Weight

B. Percent Liver Weight

Figure 2 –. Morphological measurements demonstrate differences in body weight and hepatomegaly in *Phkg2*$^{-/-}$ mice.

(A) Body weight. Total body weight was measured for WT and KO mice at 1 month, 2 months, and 3 months of age. At 1 month, KO mice have significantly lower body weight than WT controls. 1 month 20 WT (13 female, 7 male), 20 KO (13 female, 7 male). 2 months 14 WT (7 male, 7 female), 14 KO (7 male, 7 female). 3 months 14 WT (7 male, 7 female), 14 KO (7 male, 7 female). Mean with SEM. ***p<0.001. *(B) Percent liver weight*. Liver weight (LW) was measured and normalized to body weight (BW) as a quantitative marker of hepatomegaly. Percent liver weight was significantly higher in KO mice compared to WT controls. 17 WT (7 male, 10 female), 17 KO (7 male, 10 female). Min to max demonstrating all points. ****p < 0.0001.
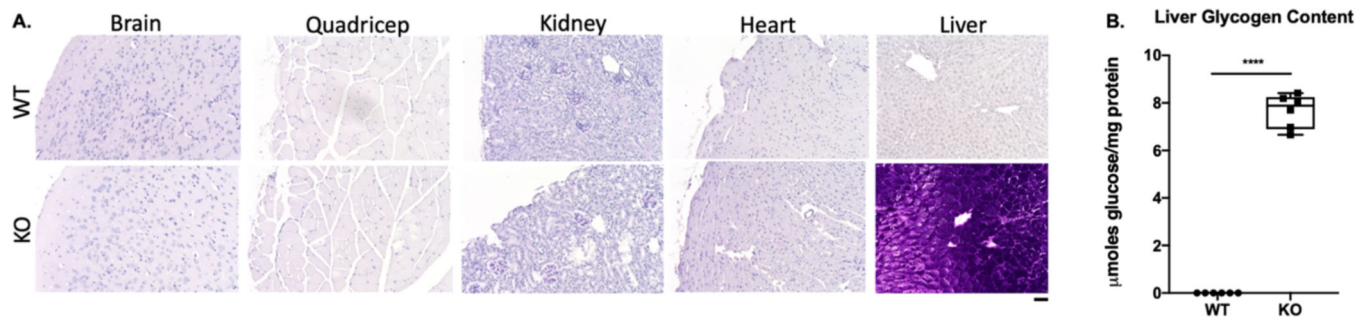
Figure 3 –. Glycogen level was significantly elevated in liver of *Phkg2*$^{-/-}$ mice and similar to WT in other tissues. (A) *PAS Stain*.
Slides were stained with Periodic acid-Schiff (PAS) to identify the presence of glycogen in tissues. Brain, quadricep, kidney, and heart tissue demonstrated no differences on PAS stain between KO mice and WT controls. Liver tissue demonstrated a remarkable difference on PAS stain between KO mice and WT controls. Images were captured at 20x. Scale bar is 50 μm. *(B) Liver glycogen content assay*. To verify PAS stain, glycogen assay was performed on liver lysates from WT and KO mice. Liver tissue from KO mice demonstrate significantly higher glycogen content levels than WT controls. Male and Female. 6 WT (3 male, 3 female), 6 KO (3 male, 3 female). Min to max demonstrating all points. ****p < 0.0001.
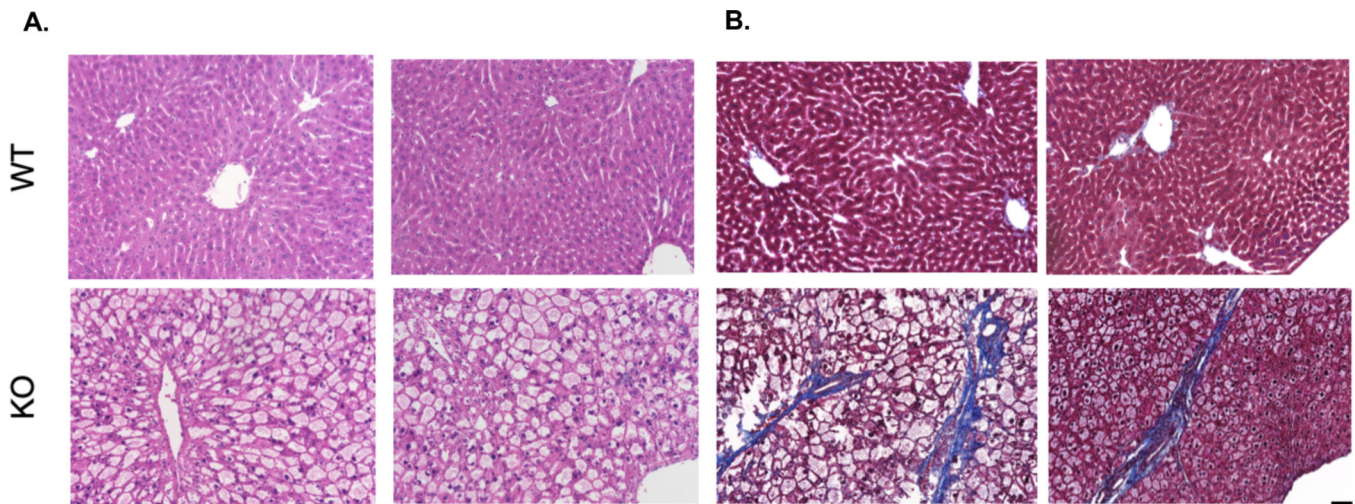
Figure 4 –. *Phkg2*$^{-/-}$ **mice demonstrated characteristic GSD hepatocyte architectural changes and early perisinusoidal fibrosis.**

(A) H&E Stain. Slides were stained with Hematoxylin & Eosin (H&E) to identify hepatocyte architecture. Per pathologist review, KO mice demonstrated heterogeneously enlarged hepatocytes with pale cytoplasm and distinct cell membranes as well as lateralized, pyknotic nuclei. 6 WT (4 male, 2 female), 5 KO (2 male, 3 female). 2 WT and 2 KO mice displayed. *(B) Masson's Trichrome Stain*. Slides were stained with Masson's Trichrome to identify tissue fibrosis. Per pathologist review, 3 KO mice demonstrated features of early perisinusoidal fibrosis. 6 WT (4 male, 2 female), 8 KO (5 male, 3 female). 2 WT and 2 KO mice displayed. Images were captured at 20x. Scale bar is 50 μm.
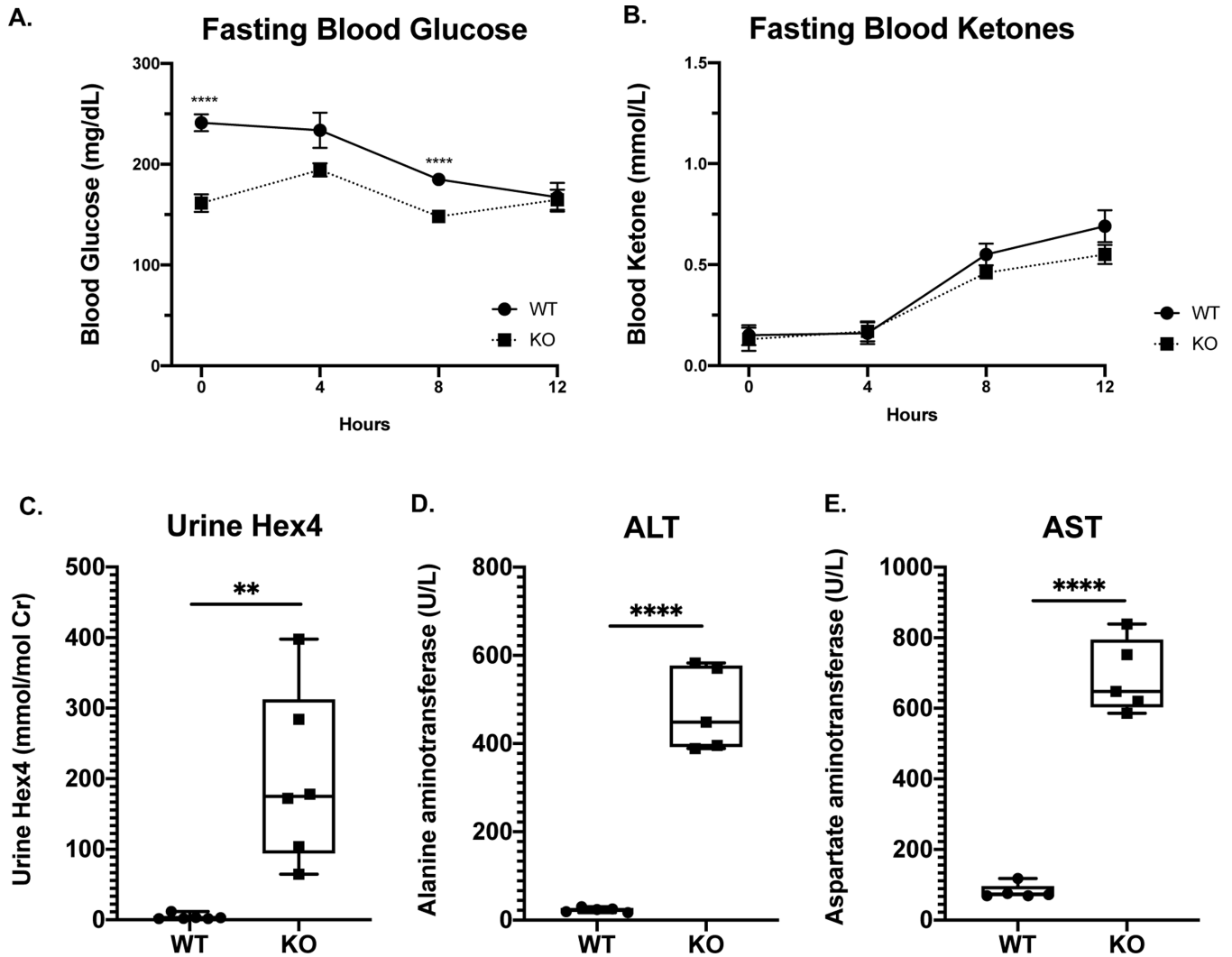
Figure 5 –. Blood and urine analyses demonstrated significantly increased ALT, AST, and Hex$_4$ levels in *Phkg2*$^{-/-}$ mice.

Fasted whole blood samples were collected to measure blood glucose and blood ketones *(A) Fasting Blood glucose curve* Blood glucose was significantly lower in KO mice than WT controls for 0 and 8 hours of fasting ****p<0.0001. *(B) Fasting Blood ketones curve* Blood ketones in KO mice were not significantly elevated compared to WT controls. 10 WT (5 male, 5 female) and 10 KO (5 male, 5 female). *(C) Urine Hex$_4$*. Urine Glc$_4$, also known as Hex$_4$, was significantly elevated in KO mice compared to WT controls. 6 WT (3 male, 3 female), 6 KO (3 male, 3 female). **p<0.01. *(D) ALT* Alanine aminotransferase (ALT) was significantly elevated in KO mice compared to WT controls ****p<0.0001. *(E) AST* Aspartate aminotransferase (AST) was significantly elevated in KO mice compared to WT controls ****p<0.0001. 5 WT (2 male, 3 female), 5 KO (2 male, 3 female). Min to max demonstrating all points.